Back-face Dynamic Profiling System: A Tool for Behind-Armour Blunt Trauma

A. Goertz[1], A. Dannaoui[2], A. Brown[3], D. Sherman[2], C. Bir[2], and K. Rafaels[4]

[1]*SURVICE Engineering Company, 4695 Millennium Drive, Belcamp, MD 21017, USA*
alan.goertz@survice.com
[2]*Wayne State University, 818 W. Hancock, Detroit, MI 48201, USA*
[3] *U.S. Army Combat Capabilities Development Command Army Research Laboratory, 800 Park Office Dr, Research Triangle Park, NC 27709, USA*
[4]*U.S. Army Combat Capabilities Development Command Army Research Laboratory, Aberdeen Proving Ground, MD 21005, USA*

Abstract. Armour back-face dynamics are responsible for injuries sustained by the wearer during non-penetrating ballistic impacts. Capturing armour back-face dynamics has been an ongoing challenge for researchers. Body armour is intended to be worn and tested with a tight fit, which visually obscures the armour back-face, and the visible armour front-face dynamics may not reflect the armour back-face dynamics. A novel Back-face Dynamic Profiling System (BFDPS) for measuring three-dimensional (3-D) dynamic armour deformation has been developed that consists of a slim fixture that is positioned between the armour back-face and surrogate or test device. The BFDPS allows for calculation of the dynamic deformation of a visually obscured rectangular fibre grid using high-speed video motion tracking of the fibre ends, which extend beyond the armour. Considering all the fibre displacements simultaneously provides constraints for an optimisation that solves for the out-of-plane displacements of the intersecting points of the fibre grid for each frame of the video. Optimisations of sequential video frames are combined to provide back-face dynamics. To assess the accuracy of the BFDPS, a ballistic experiment was conducted using a .45 ACP (Automatic Colt Pistol) bullet striking a soft armour panel backed by a transparent ballistic gelatine block. The experimental back-face dynamics were captured using motion-tracking of the high-speed video of the armour back-face profile intruding into the gelatine block. Similarly, the BFDPS fibre-grid tip displacements were tracked with high-speed video motion tracking and underwent optimisation to calculate the 3-D back-face dynamics. Superposition of the back-face profiles obtained from both methods indicate good agreement throughout the time history of the event. The promising results suggest the BFDPS has utility for tracking back-face dynamics under conditions where the back-face cannot be visually observed or measured by other means.

1. BACKGROUND

Characterising dynamic surface deformation of objects that are visually obscured by surrounding opaque surfaces is an ongoing challenge. A prime example being the measurement of the back-face dynamics of personal protective body armour, backed by clay, subjected to ballistic impact loading. Body armour is generally layered such that the dynamics of the front-facing outer armour layer are not representative of the rear back-face layer of the armour due to separation of interior armour layers. The back-face surface of the armour is normally in intimate contact with the clay so it cannot be directly observed.

Various schemes have been developed to measure 3-D shapes using thin planar sensing devices. A planar mesh using a two-layer orthogonal mesh of fibre Bragg grating (FBG) strands embedded in a 5 mm thick sheet of silicon was designed to measure 3-D shapes [1]. FBG senses strain by measuring light reflection in the fibre optic strands. This device is not well suited to ballistic armour application since the 5 mm thick gelatine would almost certainly alter the interaction between the armour back-face and the backing object. In addition, it is unlikely the fibres could withstand or accommodate large deformations that often occur in armour back-face dynamics. An FBG strand was woven into a Kevlar® body armour panel, backed by gelatine, which was impacted by a 12.59 mm steel ball with a velocity of 425 m/s [2]. The FBG slipped in the fabric so the FBG strains could not be used to determine back-face dynamics, but the strains were correlated to observed back-face dynamics determined by video through the gelatine. In follow-up studies, a method was devised to account for fibre slip by observing drops in FBG strain that allowed for estimating the back-face displacement[3, 4]. The methodology requires knowing or estimating the initial velocity of the deformation, which significantly limits the technique to environments where that is possible.

A novel fibre (wire) grid was developed, the Back-face Dynamic Profiling System (BFDPS), that uses changes in displacements of the ends of the fibres to determine changes in the shape of the grid. The grid is positioned between body armour and the body armour backing material (e.g., clay) with the fibre ends visible outside the perimeter of the armour. The fibre grid consists of flexible, low-friction, high

Distribution Statement A. Approved for public release: distribution is unlimited.

https://doi.org/10.52202/081621-0034

tensile strength Nitinol wires. The grid has a low resistance to out-of-plane deformation and therefore should have a minimal influence on the back-face dynamics. As the armour back-face deforms under impact, the free ends of the grid wires (outside the grid) are pulled into the grid to accommodate the geometric expansion of the back-face in deformation. The shape change of the grid is determined by tracking, currently with high-speed video, the linear dynamics of the free ends of the wires, which reside outside the periphery of the armour and are visible to the high-speed camera(s). The shape of the obscured grid is calculated by solving a constrained optimisation problem where the unknown Z-displacement (deformation) of each interior wire grid intersection is shared between and defined by four adjacent trapezoids, two in the X-direction and two in the Y-direction, all with known grid base lengths, which are the length of the initial grid (Figure 1). A proprietary Python™ optimisation program solves for a best-fit deformation contour that matches the observed free-end wire displacements at each camera frame, which provides the back-face dynamics when the camera frames are concatenated. The optimisation algorithm was verified by calculating a theoretically fibre pull-in history from a simulated BABT event and confirming the optimisation program's reconstruction matched the simulation results.

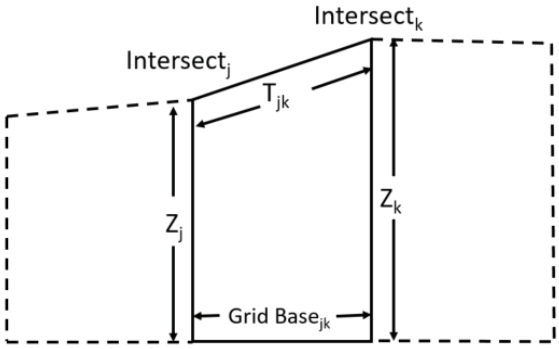

Figure 1. Wire intersection right trapezoid. Intersect$_j$ and Intersect$_k$: wire intersections; T_{jk}: deformed spanning oblique segment; Grid Base$_{jk}$: plane projected undeformed spanning segment; Z_j and Z_k: deformed wire intersection heights.

2. METHODOLOGY

A ballistic experiment with a BFDPS fixture positioned between a soft armour panel and a clear gelatine block was conducted to assess the predictive accuracy of the BFDPS compared to the armour back-face deformation observed through gelatine. Two high-speed video cameras recorded a .45 ACP bullet striking a soft armour panel, one view facing the striking surface of the armour to capture the BFDPS wire dynamics and a second side view capturing the armour back-face intrusion into the gelatine.

2.1 BFDPS Fixture

A 71 cm × 56 cm muslin fabric (Ticking Solid Natural Colour Cotton Fabric, Walmart) was used as the base material. The warp and weft of the fabric are unknown, but it has a weight of 0.23 kg/m^2. A 22 × 22 grid of 1 cm squares was drawn in the centre of the fabric. A 1 mm leather hole punch was used to create weaving holes at the grid line intersections. Non-intersecting diagonal stress relief cuts of approximately 2 cm in length were introduced into the fabric to reduce tension in the fabric during deformation, which also diminish the influence of the fabric properties on the BFDPS response. Round 0.04 cm diameter super elastic Nitinol wire (Kellogg's Research Labs, New Boston, New Hampshire) was cut into twenty-three, 51 cm sections for vertically oriented wires and another twenty-three sections of 61 cm in length for horizontally oriented wires. The wires were woven in alternating over-under patterns, skipping every other hole, through the weaving holes with the grid centred in the length of the wires for both orientations. To maintain wire alignment outside the grid, the wires were anchored to the fabric approximately 9 cm from the free end using a combination of fabric weaves and 32 cm Nitinol wires acting as straps. The wires were inserted through sections of 0.15 cm inner diameter silicon tubing between the grid and the outer alignment anchors. The silicon tubes were fastened together using gaffer's tape to keep the tubing and wires aligned during ballistic loading (Figure 2).

https://doi.org/10.52202/081621-0034

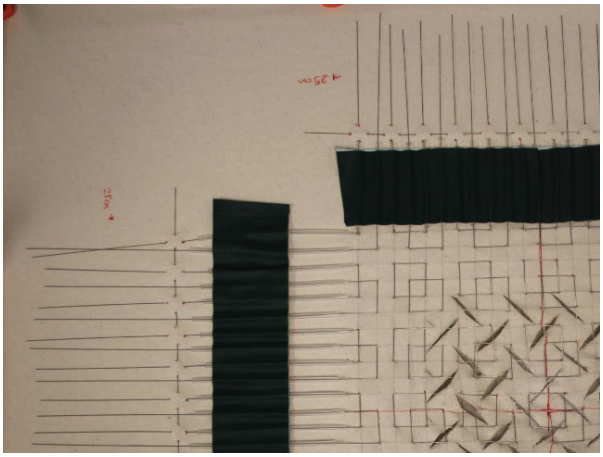

Figure 2. Quarter view (upper-left quadrant) of the BFDPS fixture.

2.2 Experimental Protocol

The chamber and barrel (.45 ACP Velocity, M34917, H-S Precision Inc) were securely mounted to a universal receiver. The barrel's end was positioned 152.4 cm from the BFDPS. The universal receiver, equipped with a remote firing mechanism, used compressed air to activate the firing pin. A full metal jacket (FMJ) round (0.45 ACP FMJ 230 grain, Q4170, Winchester) was used for this test. Three sight-in shots were fired to warm the barrel and verify the point of aim.

A 20% Clear Ballistics® gelatine block (20% NATO block, Fort Smith, Arkansas) served as the witness material. Rafaels et al. previously described the mounting fixture for the gelatine block [5].

Two high-speed cameras were employed for video capture: a Phantom® V1212 (Vision Research Inc., Wayne, New Jersey) for the lane view to visualize the BFDPS and an HX-3 (NAC Image Technology, Yokohama, Japan) for the perpendicular side view to visualize the bullet pre-impact and the back-face signature in the gelatine. Both cameras were equipped with 2.4–8.5 cm Nikon lenses (Nikon, AF Nikkor, Melville, New York) and recorded at 20,000 frames per second (FPS). The software for the V1212 and HX-3 are PCC 3.6 (PCC 3.6, Vision Research Inc, Wayne, New Jersey) and MLink (MLink x64, NAC Image Technology, Yokohama, Japan), respectively. Yellow Jacket LED lights (YJ5X, Crash Lab Support, Howell, Michigan) were positioned to backlight the gelatine block and illuminate the BFDPS, ensuring both were fully visible in the recorded videos. A 15 cm × 15 cm woven sheet of Kevlar® was positioned on the face of the gelatine block to protect it from damage from the wires.

The BFDPS fabric was clamped tautly onto a wooden frame. The clamping process involved aligning the long and short edges of the fabric and securing it with 12 small ratcheting bar clamps. The BFDPS and wooden frame were then mounted and secured using straps, with careful alignment to ensure the system's centre corresponded with the block's centre. The soft armour shoot pack was mounted onto the BFDPS (Figure 3), and the entire setup was centred using a laser. Before testing, pre-test images with a photo scale were taken. These images included the gelatine block's face, the overall setup from the lane view, close-ups of the mounted fixture, and a perpendicular view of the system. A final review of the setup ensured alignment and lighting. The V1212 camera recorded the lane-view from the point the bullet exited the barrel until the wires stopped moving post-impact, typically spanning 0.015–0.02 s. The HX-3 camera captured the side-view event from three frames before impact until the back-face deformation into the gelatine reached its maximum.

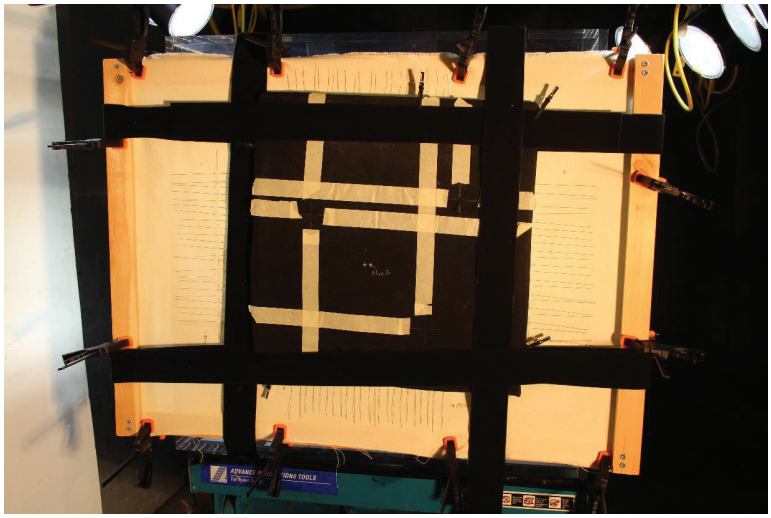

Figure 3. Assembled BFDPS with 12 ratcheting bar clamps keeping the fabric taut and hook-and-loop fastener straps holding the armour up to the fabric.

2.3 Post-processing Protocol

The high-speed video motion capture analyses for the lane and the perpendicular side camera views utilised Tracker software (Tracker 6.0.8, Open-Source Physics Project). The analysis of the lane camera view provided the positional X and Y coordinates of the BFDPS wire tips for each video frame of the analysis (Figure 4), which were subsequently used to calculate the wire tip "pull-in" displacements. An in-house custom Python™ program was used to read the Tracker motion capture analysis and solve a series of optimisation problems, one per video frame, that predicts the armour back-face contour based on the amount of wire pull-in for each wire in the BFDPS grid. To assess the profile's accuracy, the armour back-face deformation into the gelatine was also tracked.

The perpendicular side camera view provided the Y and Z coordinates of the armour back-face deformation profile (Figure 5). The armour deformation side profile history was measured along 11 lines parallel to the shot line, spaced 10 mm apart, resulting in a 100 mm profile height centred about the shot line, which was adequate for capturing the height of the back-face deformation profile. For frames where the margin of the gelatine deformation, or the wire tips for the front view, were excessively blurred or there was no detectable movement, point measurements were skipped and the coordinates were computed using the Tracker software's linear interpolation. In addition, the side camera view also provided images of the threat, prior to impacting the armour, which were used to estimate the initial threat velocity.

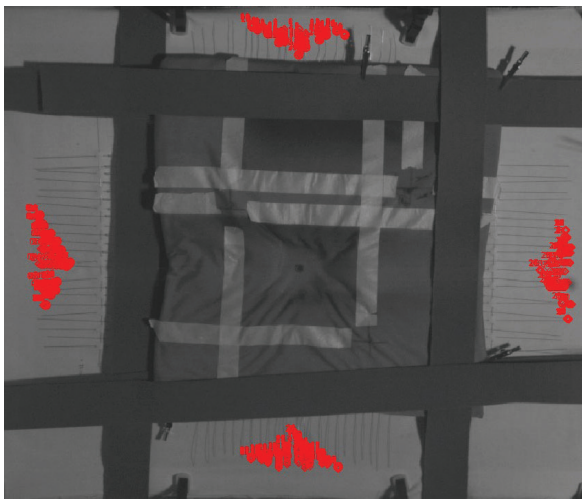

Figure 4. Tracker motion capture analysis of the lane camera view.

https://doi.org/10.52202/081621-0034

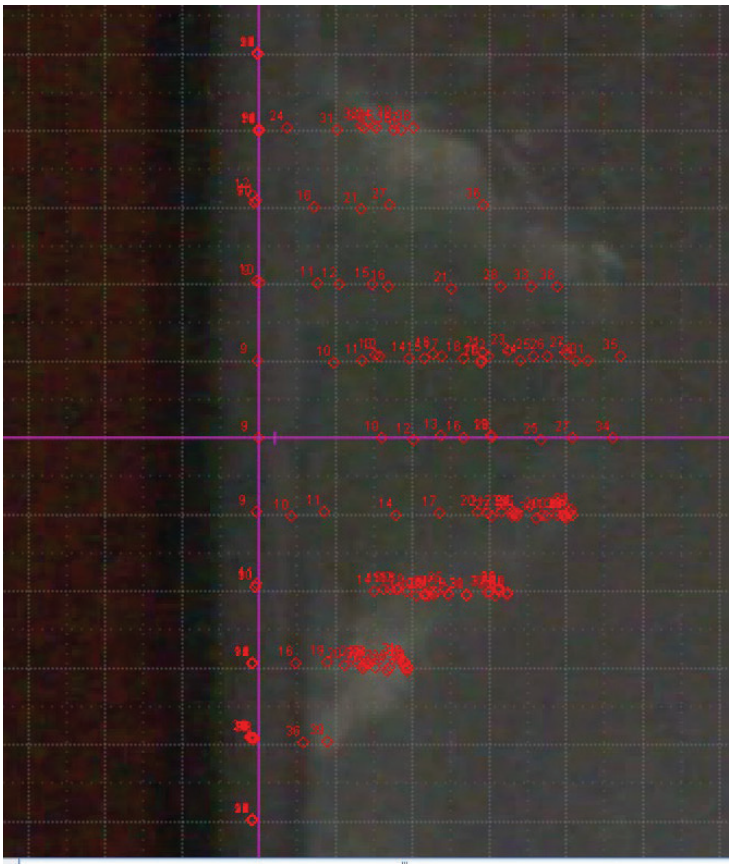

Figure 5. Tracker motion capture analysis of the perpendicular side camera view. Purple axes identify shot line and initial back-face plane.

3. RESULTS AND DISCUSSION

The motion capture analysis of the threat prior to striking the armour indicated its velocity was approximately 228 m/s at impact. The motion capture and contour optimisation analyses for the lane view video were used to generate a peak displacement history, defined by the maximum displacement of the 3-D contours of the back-face deformation for each frame of the video (Figure 6). The side view motion capture analysis generated a displacement history, also defined by the peak displacement history and a profile history. The peak displacement comparison (Figure 7) for this study was plotted through 1.4 ms, when the BFDPS analysis indicated that the armour back-face was no longer demonstrating meaningful displacements per time step. The velocity histories for both analyses were calculated using the derivative of the displacement histories and plotted (Figure 8).

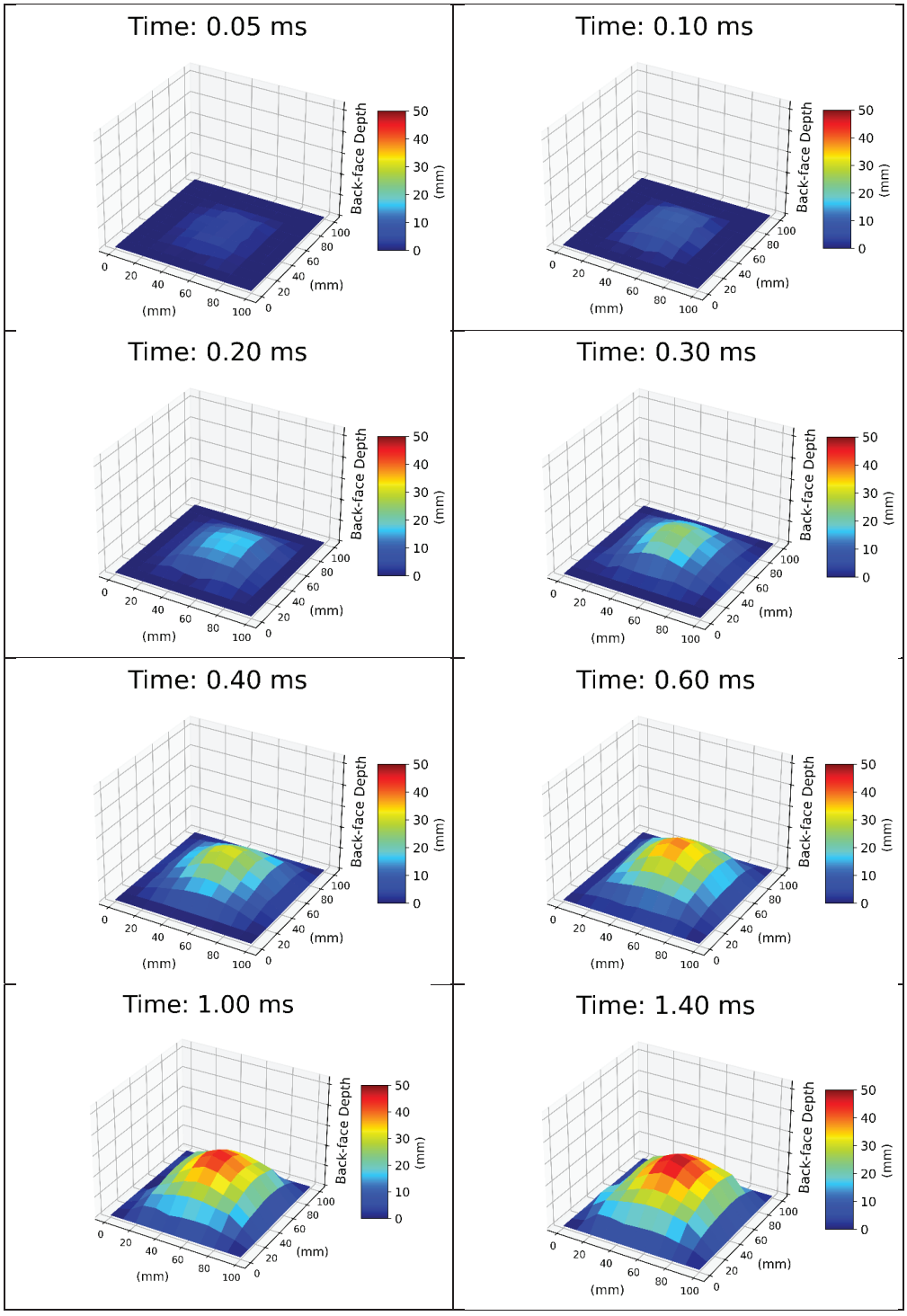

Figure 6. BFDPS-predicted back-face deformation progression.

https://doi.org/10.52202/081621-0034

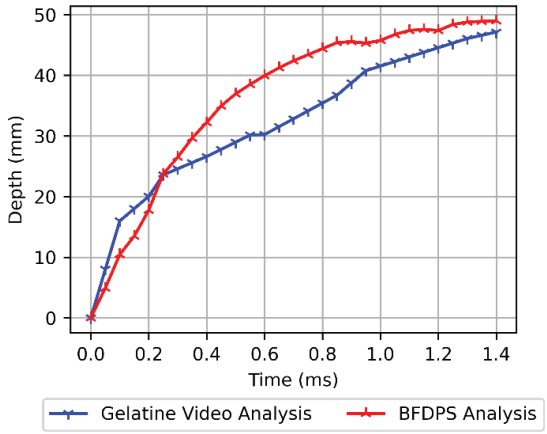

Figure 7. Peak back-face displacement histories for the gelatine video analysis and the BFDPS analysis.

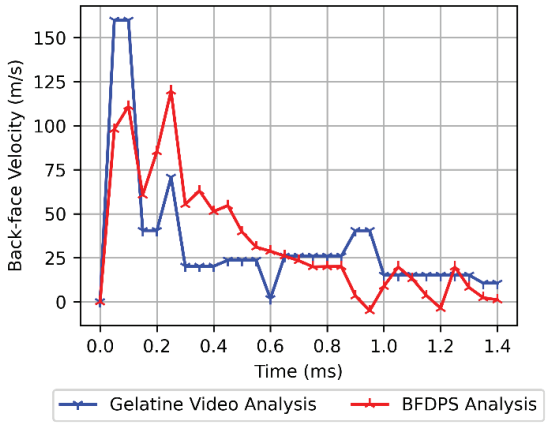

Figure 8. Peak back-face velocity histories for the gelatine video analysis and the BFDPS analysis.

The predicted BFDPS displacement history was in reasonable agreement with the gelatine displacement history through 225 μs, when the BFDPS displacements diverged from the gelatine displacements. In-house simulations of ballistic impacts to biological specimens indicate the armour back-face is largely disengaged with the surrogate at 200 μs, which is before the BFDPS displacements diverge from the backing in this study. Therefore, from a biomechanics standpoint, it appears early armour back-face dynamics are critical with respect to injury outcome since armour dynamics after separation from the backing are largely irrelevant.

In the authors' experience, the backing used in ballistic experiments, in this case gelatine, commonly separates from armour backing as the retarding mechanisms built into protective armour slow the armour back-face, while the inertia imparted to the backing during initial back-face loading continues to drive the backing material. The shape of the displacement curves in this analysis reflects those characteristics (i.e., a decelerating armour back-face and a relatively constant post-impact velocity for the gelatine backing). However, at later times, the BFDPS estimates greater displacements than the gelatine, which is contrary to what would be expected. Some of the error in calculating the displacement in the gelatine could result from optical distortion of the gelatine as it is deforming. Another reason the BFDPS could predict larger displacements than witnessed in the gelatine may be due to extraneous deformation in the wires that artificially increase the observed wire pull-in. Video analysis of other experiments has indicated that the armour may separate from not only the gelatine but also the BFDPS at later times, such that the wires can exhibit inertially driven displacements as well (Figure 9).

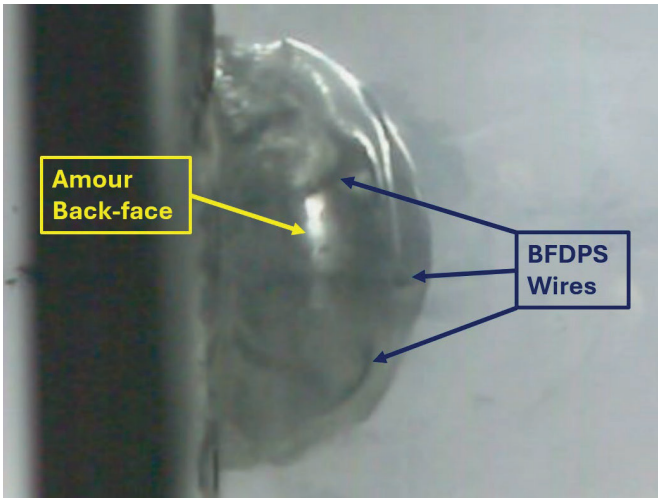

Figure 9. Example of armour and BFDPS wires separating from a hard armour plate.

The comparison of the back-face velocity predictions from the analyses confirms that derivations of dynamic histories are notoriously noisy [6-8]. The back-face velocity history for the gelatine analysis suggests approximately 160 m/s peak back-face velocity, which is reasonable given the estimated 228 m/s threat impact velocity and the resolution of the analysis (25 μs). The BFDPS analysis peak velocity occurred at 225 μs, which is unreasonable. This suggests that the early displacement estimates for the BFDPS were low. An adjustment manually overriding the optimisation analysis while maintaining a constant area under the velocity trace to preserve the later BFDPS displacement estimates might improve the consistency between the gelatine and BFDPS displacement histories prior to 225 μs.

https://doi.org/10.52202/081621-0034

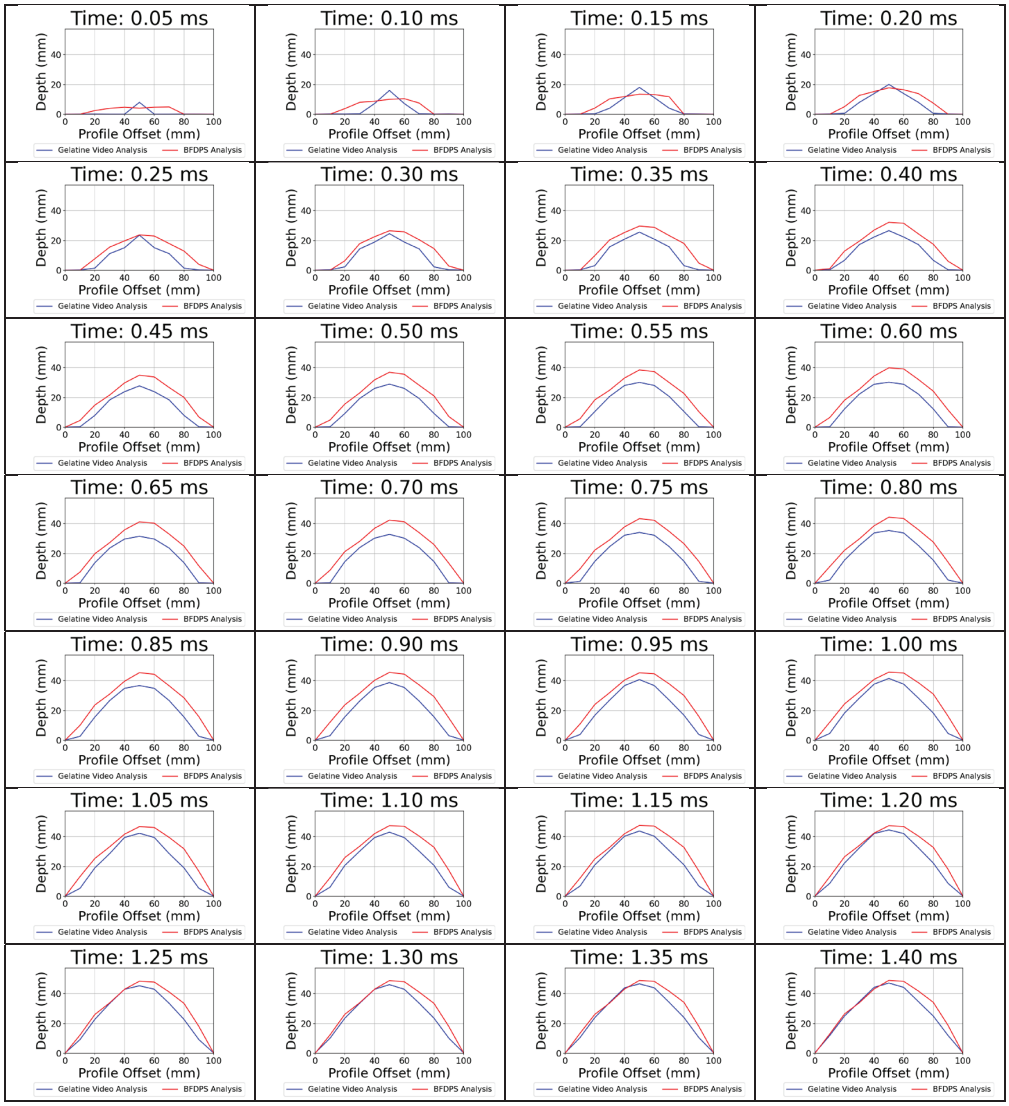

Figure 10. Profile histories comparing the gelatine video (blue) and the BFDPS (red) analyses.

The profile history comparisons between the gelatine and BFDPS analyses are shown in Figure 10. The BFDPS optimisation depicts an initially wider and shallower deformation profile than the gelatine analysis. It is noteworthy that the camera view of the BFDPS showed movement over a 70 mm span (a span containing six wires), while the gelatine analysis showed movement over a 20 mm span (a span containing the equivalent of only one wire). Although strain relief cuts were introduced into the BFDPS weaving fabric, it is possible that once a single wire of the BFDPS was loaded by the armour, ancillary loading paths through the BFDPS fabric and grid could induce anomalous wire movement of neighbouring wires not yet directly deformed by the armour back-face. Beyond the relatively coarse initial profile shapes, the BFDPS profile shape tracked the gelatine well.

The BFDPS does have limitations. The BFDPS cannot detect or represent deformation that is undercut (e.g., mushroom capping) or purely vertical. The resolution of the BFDPS is limited to the spacing of the grid fibres, which itself is practically constrained by frictional binding when fibres are too closely spaced, and the temporal resolution of the high-speed cameras. Frictional binding can be reduced by increasing the spacing between over-under weaves, if implemented. The BFDPS wire thickness may need to be adjusted to accommodate changes in back-face loading profiles. For example, the researchers in this study found they had to increase the wire sectional size as the threat level and anticipated response increased to prevent damaging the wires. In cases where there are substantial strains in the back-face surface, the fibre intersections may deviate laterally during back-face deformation, particularly when

large back-face strains are present. The optimization algorithm does specifically not account for potential lateral offsets, which is an area for future consideration.

4. SUMMARY

This experiment and analysis demonstrated a novel method for capturing 3-D contour histories of surfaces that may be completely visually obscured. Capturing the dynamic profile is important for understanding the potential for injury behind armour systems [9]. This method fills a current gap for behind-armour blunt impact injury researchers who are essentially blind to the insulting dynamics of the armour back-face during a ballistic impact that is backed by an opaque backing material. It uses readily available, low-cost materials, other than a high-speed camera, which many ballistic facilities already possess. This study demonstrated the concept using a handgun threat impacting soft body armour. Subsequent testing by the authors has shown the system has utility with rifle threats impacting more robust armour systems. Those findings are beyond the scope of the present study and warrant a separate report.

Acknowledgments

The authors would like to thank Robert MacDonald for his testing expertise and support throughout the development of the BFDPS.

The research reported in this document was performed in connection with contract/instrument W15P7T-19-D-0126 with the Combat Capabilities Development Command (DEVCOM) Army Research Laboratory.

The findings in this report are not to be construed as an official Department of the Army position unless so designated by other authorized documents. The views and conclusions contained in this document are those of SURVICE Engineering Company, LLC and the DEVCOM Army Research Laboratory.

Conflicts of interest: The BFDPS is under patent pending by SURVICE Engineering Company, LLC with authors A. Goertz, A. Brown, and K. Rafaels as co-inventors.

References

[1] L. Xu, J. Ge, J. H. Patel, and M. P. Fok, Dual-layer orthogonal fiber Bragg grating mesh based soft sensor for 3-dimensional shape sensing, *Optics Express,* vol. 25, no. 20, pp. 24727-34, 2017.

[2] D. A. Hackney, T. Goode, F. Seng, S. Schultz, M. Pankow, and K. Peters, In-situ strain measurement of ballistic fabrics during impact using fiber Bragg gratings, *Optical Fiber Technology,* vol. 59, pp. 1-9, 2020.

[3] F. Seng *et al.*, Dynamic back face deformation measurement with a single optical fibre, *Int J of Impact Engineering,* vol. 150, pp. 1-9, 2021.

[4] I. Velasco, P. Spackman, and S. Schultz, Body armor shape sensing using fiber Bragg gratings, presented at the Intermountain Engineering, Technology and Computing (IETC), 2020.

[5] K. A. Rafaels, K. Choi, G. Glasser, and C. Bir, "Estimation of Armour Backface Velocity," in *Proceedings of the Personal Armour Systems Symposium 2020*, Copenhagen, Denmark, Oct 11-15, 2021.

[6] D. A. Murio, Automatic numerical differentiation by discrete mollification, *Computers & Mathematics with Applications,* vol. 13, no. 4, pp. 381-386, 1987.

[7] F.-F. Dou, C.-L. Fu, and Y.-J. Ma, A wavelet-Galerkin method for high order numerical differentiation, *Applied Mathematics and Computation,* vol. 215, no. 10, pp. 3702-3712, 2010.

[8] T. Wei, Y. C. Hon, and Y. B. Wang, Reconstruction of numerical derivatives from scattered noisy data, *Inverse Problems,* vol. 21, no. 2, p. 657, 2005.

[9] K. A. Rafaels, "Importance of Areal Measurements for Thoracic BABT Test Devices," in *Proceedings of the Personal Armour Systems Symposium 2016*, Amsterdam, Netherlands, Sep 19-23, 2016.

https://doi.org/10.52202/081621-0034